

Uniform foam production by turbulent mixing: new results on free drainage vs. liquid content

A. Saint-Jalmes, M.U. Vera, and D.J. Durian

UCLA, Department of Physics and Astronomy, Los Angeles, California 90095-1547, USA

Received 15 February 1999

Abstract. An apparatus is described for rapidly producing large quantities of foam *via* turbulent mixing of gas with a narrow jet of a surfactant solution inside a delivery tube. By controlling relative flow rates, the gas volume fraction in the resulting foam may be easily varied across $0.3 < \phi < 0.99$. Using such foams, we present a comprehensive set of data for free drainage as a systematic function of gas fraction and sample geometry. The qualitative behavior can be understood in terms of simple theoretical considerations, emphasizing the importance of controlling the initial foam conditions. Quantitative features are compared with two approximate versions of the drainage equation, highlighting the crucial role of capillarity for very dry foams and small samples.

PACS. 82.70.Rr Aerosols and foams – 47.60.+i Flows in ducts, channels, nozzles, and conduits – 47.55.-t Nonhomogeneous flows

Introduction

Aqueous foams are familiar from everyday life in foods, cosmetics, and detergents. While appearing creamy and white from a distance, they consist of macroscopic gas bubbles tightly packed in a relatively small volume of surfactant solution [1–5]. As a form of matter, foams exhibit unusual mechanical properties based on the tight packing and rearrangement dynamics of the bubbles [6–8], being able to support nearly static shear like a solid and yet able to flow and deform like a liquid. Combined with low density and high interfacial area, this provides the basis for a host of unique industrial applications such as firefighting and separating, isolating, or spreading chemicals or particles. A primary concern wherever foams occur is their stability. With time, they evolve by some combination of three basic mechanisms: bubble coalescence *via* film rupture; coarsening *via* diffusion of gas from smaller to larger bubbles; and drainage of the liquid downwards and out from the foam in response to gravity. While coalescence can be prevented by suitable use of surfactants, and while coarsening is quite well understood [9–12], drainage remains a basis and applied research topic of active interest [13,14]. A very productive line of recent study concerns the response to forced addition of liquid from the top. This includes such intriguing behavior as solitary waves [15], structural transitions [16], and convective instabilities [17].

In this paper we are concerned with a more traditional problem: the free drainage of liquid out from an initially uniform column of foam, without forced addition of liquid. In spite of its obvious importance and long study, this remains an outstanding problem. Theoretically, this is in

part because the drainage equation is nonlinear and cannot be solved analytically. Experimentally, this is in part because of the close coupling of drainage with film rupture and coarsening, but more because of uncontrolled foam production methods. Here, to avoid the latter difficulty, we describe an apparatus that allows rapid production of uniform foams with very small bubbles. After reviewing the theory of foam drainage, we present new free drainage data as a systematic function of the liquid content of the initial foam. This permits clean quantitative comparison with drainage equation predictions.

Turbulent foam production

Aqueous foams may be produced by many techniques. The most familiar, perhaps, is simply to vigorously shake a closed container partially filled with surfactant solution. The aerosol method is also familiar in consumer products such as shaving cream, hair styling mousse, and whipped cream [18]. Another popular method is to bubble gas directly into a standing pool of surfactant solution. In fact, this is used in most drainage studies of which we are aware. Since the bubbling method is slow, the liquid solution drains significantly during production, giving foams which are drier at top and wetter at bottom. The subsequent drainage depends crucially, of course, on this initial non-uniformity. To avoid the resulting ambiguities, we have constructed a simple apparatus based on firefighting technology in which a high-speed jet of solution mixes with a stream of gas. This method allows us to produce large volumes of uniform foam rapidly, with a liquid content that is easily varied.

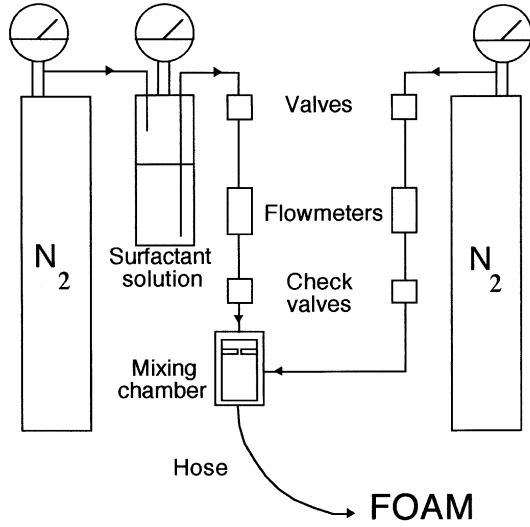


Fig. 1. Apparatus for the production of foam. Surfactant solution is forced through a small hole in the mixing chamber, where the resulting jet mixes turbulently with a continuous supply of gas. By controlling the liquid:gas flow rates, the liquid content of the foam may be chosen as desired.

Our apparatus is depicted schematically in Figure 1. Similar devices are described in references [19,20]. Large-scale versions are available commercially to generate foams for covering landfills, spreading fertilizers or pesticides, etc. [21]. The heart of the apparatus is a cylindrical brass mixing chamber, length 5 cm and inner diameter 0.5 cm, into which both gas and solution are metered at steady rate. To force liquid into the chamber, the gauge pressure in a reservoir is raised to about 120 PSI by a bottle of compressed N_2 . This produces a powerful jet of liquid through a tiny hole in the center of the chamber, 0.7 mm diameter and 2 mm long, with a liquid flux of $15 \text{ cm}^3/\text{s}$ and a corresponding average speed of 4 000 cm/s. To produce foam, gas is simply fed into the jet-side of the chamber, which is at roughly 80 PSI. Note that the Reynolds number based on jet speed, chamber diameter, and liquid viscosity is $vD/\eta = 2 \times 10^5$; this is sufficiently large for turbulent mixing of gas and liquid into a smooth foam with very fine bubbles. Note also that the capillary number based on jet speed, liquid viscosity, and interfacial tension is $\eta v/\sigma = 1$, suggesting that viscous stresses can overcome surface tension and hence rip apart large bubbles. Metering valves, flowmeters, and check valves are used in both supply lines in order to control and measure the relative gas:liquid flow rates, and to prevent mishaps.

The mixing chamber dimensions and operating pressures were chosen by trial and error, but are not critical. However, once these are fixed, the deliver hose on the downstream side of the chamber must be chosen accordingly with great care. If it is too short, then the gas and liquid do not thoroughly mix; if it is too long, then a sputtering instability occurs in which smooth slugs of foam are punctuated by large pockets of unmixed gas. We speculate that the optimal length of hose is determined by the remaining gauge pressure and the flow resistance

Table 1. The surfactant solution in our experiments consists of 0.4%, by weight, of AOS (α -olefin sulfonate) in water. The resulting solution, foam, and drainage properties are tabulated here. Note that the maximum possible Plateau border area is computed, giving the maximum characteristic liquid flow speed V (assuming Plateau border-dominated viscous dissipation), and the minimum capillary length ξ . The surface viscosity was measured [36] from linear response in a two-dimensional Couette viscometer [37] operating at 0.04 Hz; systematic errors may be present due to operation near the limit of sensitivity, but the quoted number represents a firm upper bound.

quantity	value
ρ , solution density	1 g/cm ³
η , bulk viscosity	0.011 g/cm-s
η_s , surface viscosity	0.008 ± 0.002 g/s
γ , surface tension	44 erg/cm ³
R , bubble radius	55 μm
$A = (CR)^2$	490 μm^2
$V = \rho g A / \eta^*$	1.7 mm/min
$\xi = C\gamma / 2\rho g A^{1/2}$	4.1 cm

per unit length of foam, such that the foam speed in the hose is commensurate with the input streams and required mixing times. As a practical matter, we simply start with a long delivery hose and progressively cut it as necessary. For our 3 mm inner diameter hose, a length of 1.5 m works well; for larger diameters, longer lengths are needed.

For all the experiments presented here, we used an aqueous solution of AOS (α -olefin sulfonate, Witco Corporation) with concentration of 0.4% by weight, slightly smaller than the critical micelle concentration. The physical properties relevant to drainage are recorded in Table 1. With this solution and our apparatus, we are able to produce uniform foams with gas fractions continuously variable across the range $0.3 < \phi < 0.99$, with a reproducibility of better than 1%. The production rate depends on liquid content, but is typically about $100 \text{ cm}^3/\text{s}$ of foam. The bubble size distribution may be estimated by optical microscope observation of surface bubbles against glass. Independent of ϕ , it is peaked around an average diameter of 110 μm , presumably the limit below which the jet of solution may no longer break up a bubble into smaller ones. The polydispersity is not great, with roughly 60% of the bubble diameters between 80 and 130 μm , and seemingly no bubbles smaller than 20 or larger than 190 μm .

Drainage experiments

The traditional drainage experiment is to measure the height $L(t)$ of drained liquid underneath a sample [1,22–24]. However, as recognized recently [25,26,14], even this simple measurement is not without ambiguity owing to an uncontrolled initial distribution of liquid throughout the foam. This problem arises because the production method, where bubbles are produced within a standing solution, is slow and coupled intimately with the drainage process; this results in a irreproducible foam which is significantly

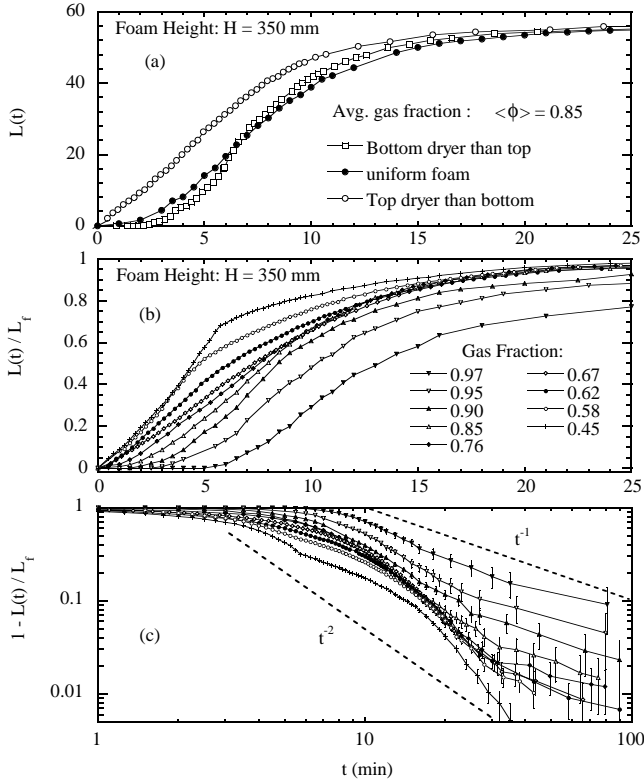


Fig. 2. Height of drained liquid underneath a foam *vs.* time after production for (a) nonuniform initial liquid content and (b,c) uniform but variable initial liquid content. The latter are normalized by the final liquid height, $L_f = L(\infty)$.

wetter at the bottom than at the top. With our method of foam production by turbulent mixing, we may neatly avoid all such problems. The importance of doing so is illustrated by the raw $L(t)$ data in Figure 2a for three different foams, each with the same average gas fraction of $\langle \phi \rangle = 0.85$. In addition to a uniform foam, we have created samples which are wetter or drier at bottom simply by smoothly varying the relative gas:liquid flow rates into the mixing chamber during production. As seen in Figure 2a, the initial liquid distribution significantly affects the drainage behavior: when wetter at the bottom, the initial drainage rate is faster and nearly constant; when dryer at the bottom, the initial drainage rate vanishes for several minutes and then increases rapidly with time. Clearly, for clean comparison with theory, it is crucial that the initial liquid distribution be controlled and known.

For uniform foams of variable initial liquid content, we display in Figure 2b typical data for the height $L(t)$ of drained liquid *vs.* time. The diameter of the foam samples is 60 mm, but identical results are obtained for diameters of 35 and 140 mm. The initial height of the foam samples is $H = 350$ mm, so we normalize the all $L(t)$ data by the final liquid height, $L_f = \lim_{t \rightarrow \infty} L(t)$, for dimensionless comparison. The results in Figure 2b show that the wetter foams drain more rapidly, of course, since the liquid channels in between bubbles are larger and hence present less hydrodynamic resistance. Also note that the initial shape of the drainage curves change systematically with

liquid content, being roughly constant for wet foams, and being flat followed by a more rapid increase for dry foams. At later times, for all foams, the drainage rates eventually decrease as L_f is approached.

How, then, would be best to quantify the differences in drainage behavior as the foam is varied? It is straightforward experimentally to measure the time t_c at which $L(t)$ has an inflection and at which the drainage rate, dL/dt , is a maximum. At this special time, it is also straightforward to measure the dimensionless liquid height $L_c/L_f = L(t_c)/L(\infty)$, and the dimensionless drainage rate $R_c = d(L/L_f)/d(t/t_c)|_{t_c}$. This generalizes and extends the practice of measuring only the time at which *half* the liquid has drained. Before showing results, we first discuss the theoretical expectations for these quantities.

Drainage equations

A minimal theory for the gravitation segregation of liquid and bubbles in a foam is reviewed in references [27,14]. The principal assumption is that all liquid flow is confined to the Plateau borders, where three neighboring bubbles meet, and that these borders have a scalloped-triangular cross section whose area A depends on the liquid volume fraction, $\varepsilon = 1 - \phi$. The relation between border area and liquid content depends on geometrical details of the bubble shapes; for dry foams it is $A = \alpha R^2$ where R is the sphere-equivalent bubble radius and α is a number between 1 and 2 [26]. The evolution of A , or equivalently ε , with time then follows from continuity,

$$\frac{\partial A}{\partial t} + \frac{\partial}{\partial z}(VA) = 0, \quad (1)$$

if the downward speed V of liquid in the Plateau borders is known as a function of A ; here $+z$ is in the direction of gravity. In references [22,14], it is argued that the liquid speed is determined by the balance of gravity, capillarity, and viscous stress from shear flow within the Plateau borders as

$$V = \frac{\rho g}{\eta^*} \left(A - \frac{C\gamma}{2\rho g\sqrt{A}} \frac{\partial A}{\partial z} \right). \quad (2)$$

Here, η^* is an effective viscosity that depends on the shape and average orientation of the Plateau borders; and $C = \sqrt{\sqrt{3}} - \pi/2 = 0.401565\dots$ relates the area and radius of curvature r of the Plateau borders according to $A = (Cr)^2$. As written, the characteristic velocity at which viscous dissipation balances gravity is recognized as $\rho g A / \eta^*$, and the characteristic length at which capillarity balances gravity is recognized as $C\gamma / 2\rho g\sqrt{A}$. Inserting equation (2) into equation (1) yields the standard drainage equation for $A(z, t)$. Though nonlinear, exact solutions are available for certain situations [28–30,27,14]. Similarity solutions may also be developed, as well as generalizations to higher dimensions [31]. Complementary numerical approaches incorporating more detailed geometrical features

and dissipation mechanisms, as well as coalescence, have also been considered, *e.g.* in references [32,13].

While the standard drainage equation appears to capture many experimental features, the form of the dissipation in equation (1) has recently been called into question [33]. If the limiting source of dissipation is due to viscous flow within the vertices, where four Plateau borders meet, rather than within the borders themselves, then the characteristic velocity set by gravity and dissipation scales as $A^{1/2}$, rather than as A in equation (2). This should hold when the surfactant monolayer is neither rigid nor viscous enough to give a no-slip condition for bulk flow, so that plug-like flow occurs within the Plateau borders and dissipative shear flow occurs only within the vertices. The resulting predictions provide better agreement for the speed of a wetting front advancing into a dry foam as the wetting rate is widely varied [33].

Whatever the dissipation mechanism, the drainage equation may be solved exactly for the final equilibrium profile of Plateau border area *vs.* depth [34,27,31]:

$$A(z) = A_H / \left[1 + (H - z)/2\xi \right]^2 \quad (3)$$

Here H is the total depth of the foam; z is measured downward from the top of the foam; A_H is the Plateau border area at the bottom of the foam; and $\xi = C\gamma/2\rho g\sqrt{A_H}$ is the scale of capillary rise of liquid upwards into the foam: $1/\xi = d(A/A_H)/dz|_H$.

The real problem of interest in this paper is how the final equilibrium is attained, starting at time zero with a uniform foam of constant Plateau border area, $A(z,0) = A_0$. Unfortunately, this “free drainage” problem is not soluble, though the drainage equation may be linearized, and similarity solutions may be developed, for behavior near equilibrium [27,31]. For very tall samples, $H \gg \xi$, it seems reasonable that capillarity, and hence the most egregious nonlinearity in the drainage equation, may be neglected throughout most of the sample. Dropping the capillary term from the standard drainage equation, in which dissipation occurs only within the Plateau borders, Kraynik [35] developed the following approximate solution:

$$A(z,t) = A_0 \begin{cases} (z/\nu_0 t) & z \leq \nu_0 t \\ 1 & z \geq \nu_0 t \end{cases} \quad (4)$$

where the speed of the drying front is $\nu_0 = 2\rho g A_0/\eta^*$, proportional to the initial liquid Plateau border area A_0 and, hence, to the initial liquid content ε_0 . At short times, the profile is linear near the top and constant near the bottom, giving a constant flow of liquid out from the foam. At long times, the profile is linear across the entire sample and the flow rate diminishes with time until, eventually, all liquid has drained. Of course since capillarity has been neglected, the Plateau border area approaches zero, rather than equation (3), at long times.

We may develop a similar solution, approximate in its neglect of capillarity, when the drainage equation is modified such that dissipation due to viscous shear flow occurs

only within the vertices:

$$A(z,t) = A_0 \begin{cases} (z/\nu_0 t)^2 & z \leq \nu_0 t \\ 1 & z \geq \nu_0 t \end{cases}. \quad (5)$$

Now, the speed of the drying front scales with the initial border area and liquid content as $\nu_0 \propto \sqrt{A_0} \propto \sqrt{\varepsilon_0}$. The only other difference is that the profile becomes quadratic, rather than linear, for $z = \nu_0 t$. At short times, near the bottom, the liquid content and drainage rate are constant as before.

In our experiments, we do not measure the liquid content or Plateau border area as a function of position and time within the foam. Rather, we simply record the height of drained liquid, $L(t)$, emerging underneath the foam. This quantity may be predicted from $A(z,t)$ either by integration across the sample or from the drainage rate per Plateau border at the bottom, $VA(H,t)$. Normalizing to the final liquid height, L_f , when all liquid has drained, the result based on equation (4) for border-dominated dissipation is

$$L(t) = L_f \begin{cases} \frac{1}{2}(\nu_0 t/H) & \nu_0 t \leq H \\ 1 - \frac{1}{2}(H/\nu_0 t) & \nu_0 t \geq H \end{cases}. \quad (6)$$

The drained liquid height is thus predicted to be continuous and differentiable, with an inflection at time $t_c = H/\nu_0 \propto H/\varepsilon_0$. At this time the liquid content at the bottom first starts to decrease, and the dimensionless height is $L_c/L_f = 1/2$, *i.e.* half of all liquid has drained. The corresponding dimensionless accumulation rate is $R_c = d(L/L_f)/d(t/t_c)|_{t_c} = 1/2$. By contrast, the drained liquid height based on equation (5) for vertex-dominated dissipation is

$$L(t) = L_f \begin{cases} \frac{2}{3}(\nu_0 t/H) & \nu_0 t \leq H \\ 1 - \frac{1}{3}(H/\nu_0 t)^2 & \nu_0 t \geq H \end{cases}. \quad (7)$$

The result is still continuous and differentiable, growing linearly at short times, but now has an inflection at time $t_c = H/\nu_0 \propto H/\sqrt{\varepsilon_0}$. At this time the dimensionless height is $L_c/L_f = 2/3$ and the dimensionless accumulation rate is $R_c = d(L/L_f)/d(t/t_c)|_{t_c} = 2/3$. By comparing these predictions with experimental data, we hope to establish the extent to which capillarity may be neglected, as well as whether viscous dissipation occurs principally within the borders or vertices.

Comparison

The first comparison we make between theory and experiment is through a space-time plot of the liquid profile within the foam. The top plot in Figure 3 depicts equation (4), with color chosen according to the local Plateau border area A , or equivalently the liquid fraction

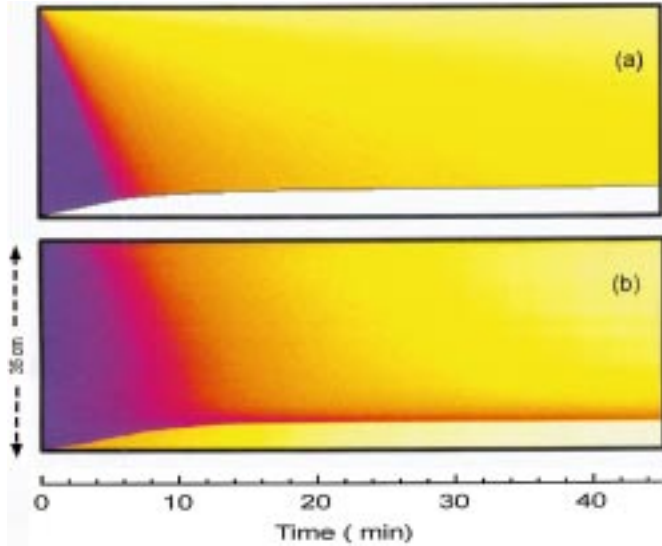


Fig. 3. Space-time plots of (a) predicted liquid content, equation (4), assuming Plateau border-dominated dissipation and neglecting capillarity, and (b) diffuse transmission of white light through an actual foam.

$\varepsilon_0 = 1 - \phi_0$. The drained liquid under the foam is indicated by white, with $L(t)$ indicated by the black line at the interface according to equation (6). The bottom plot in Figure 3 depicts experimental data for a draining foam in a rectangular tank, with color chosen according to the diffuse transmission probability for white light. Since wetter foams scatter light more strongly than dry foams, the diffuse transmission gives an indication of the liquid content (though we have not arranged the optics to make reliable calibration possible). While the two plots share much in common, there are clear differences. Most obviously, the predicted liquid content eventually vanishes while the actual liquid content approaches a capillary profile similar to equation (3); note that the scale of capillary rise of liquid into the foam agrees well with the expectation, $\xi = 4.1$ cm shown in Table 1, based on bubble size and surface tension. Another difference is that the predicted profile is a function of the single variable $z/\nu_0 t$, so that equal-color contours in Figure 3a are straight lines emanating from the upper left corner; this is true also for equation (5), or any other form of dissipation, as long as capillary effects are neglected. By contrast, the experimental equal-color contours have a different shape, indicating a more complicated dependence on position and time. This must be because, in addition to $\nu_0 t$, there is a second length scale given by the capillary rise parameter ξ . Thus, even from the qualitative features of Figure 3, we immediately see evidence of the importance of capillarity in foam drainage.

Quantitative comparisons can be made based on data for the height $L(t)$ of drained liquid. We begin by returning to Figure 2b and recalling that the initial rise of $L(t)$ is predicted to be linear in time for both border- and vertex-dominated dissipation. Experimentally, this holds only for rather wet foams, with less than about 62–64% gas by volume. For slightly drier foams, up to 80–85% gas, the initial rise in $L(t)$ appears quadratic. For even drier foams, $L(t)$

begins to rise only after a nonzero length of time following production. This range of initial behaviors is not captured by the simple approximate predictions of equations (6, 7); we argue it must be due to capillarity. To pack bubbles tighter than about 63%, random close packing, requires distortion away from the preferred spherical shape that minimizes the total interfacial free energy. Since further drying causes even further distortion and hence energy cost, it is resisted by capillary forces. Therefore, liquid may drain out from the foam only when the gas fraction at the very bottom becomes less than about 63%. This happens immediately for foams that are initially very wet, but requires finite time for foams that are initially very dry. According to this picture, the full importance of capillarity cannot be gauged by a simple comparison of foam height and capillary length.

In Figure 2c we replot the data of Figure 2b to highlight the final drainage behavior, *i.e.* the approach of $1 - L(t)/L_f$ to zero. The power-law predictions of equations (6, 7), t^{-1} and t^{-2} respectively, are indicated by dashed lines. While the dynamic range of the data is limited, it does appear that the final approach to L_f is slower than a power law. We don't believe this is due to uncertainty in the estimated values of L_f , as may be judged by the systematic error bars. We can only speculate that the slow approach is due to the delicate tradeoff between emptying excess liquid and simultaneously establishing the final capillary profile. While the simple predictions of the previous section already break down at short times for dry foams, they must also break down at late times as the capillary profile becomes established. One might still hope for some validity at intermediate times, especially for very tall samples. However, even for $H/\xi \approx 9$, we see no substantial range of power-law behavior. Forcing such a fit over a limited range of intermediate times would give results close to t^{-1} for the driest foams and t^{-2} for wetter foams. Nevertheless, we cannot clearly identify the source of dissipation from Figure 2; we can only conclude that neither equation (6) nor (7) adequately describes $L(t)$ data. It seems likely that the major source of this discrepancy is not the treatment of dissipation, but rather the neglect of capillarity.

To further explore drainage behavior and highlight the potential role of capillarity, we now examine trends as a function of the foam height, H . Rather than study the full form of $L(t)$, we instead focus on three characteristic features easily extracted from $L(t)$ *vs.* t data, namely the inflection time t_c and the corresponding dimensionless liquid height and drainage rate identified earlier. To begin, raw data for t_c is collected in Figure 4a *vs.* H for foams of various initial liquid content. Contrary to the simple predictions of equations (6, 7), the results do not tend to zero for small H , especially for dry foams, because of capillary hold-up. But at larger H , the results tend toward linearity more in accord with expectation. Curiously, though, the large- H values become independent of liquid content for foams drier than about 85% gas. This is especially puzzling because, recall, equations (6, 7) predict the scaling with height and gas fraction to be such that $t_c(1 - \phi)/H$ and $t_c\sqrt{1 - \phi}/H$, respectively, are constant.

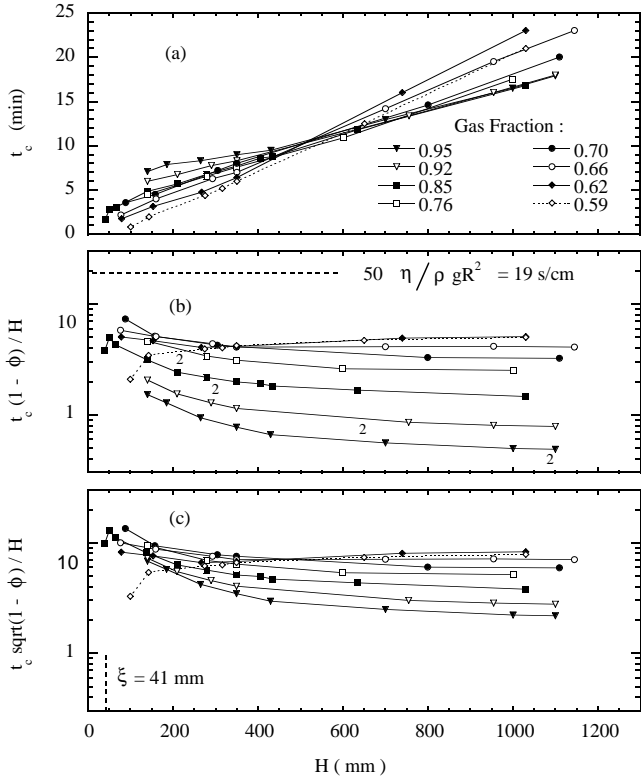


Fig. 4. (a) Time t_c at which the drained liquid height $L(t)$ has an inflection, *i.e.* at which the drainage rate dL/dt is maximum, as a function of foam sample height H . According to the approximate predictions neglecting capillarity, the results should scale with H and liquid content such that the quantities plotted in (b) and (c) are constant for Plateau border-dominated and vertex-dominated dissipation, respectively. As an aside, foams wetter than about 63% gas show qualitatively different trends in behavior since the bubbles are free to convect and rearrange.

For emphasis, we show these quantities in Figures 4b, c; evidently, neither form of scaling successfully collapses the data to a constant. For Plateau border-dominated dissipation, the predicted constant has value $50\eta/\rho g R^2 = 19 \text{ s/cm}$; evidently, the actual drainage is significantly faster. In regards to the role of capillarity, consider now the height at which t_c/H becomes constant. It can be seen from the scaling plots in Figure 4 that H must be very significantly greater than the capillary length ξ for this to occur, all the more so for drier foams. Rather than simply ξ , we propose that the correct criterion for asymptotic behavior is that much more liquid drain out than be held up in the capillary profile. From the profile of equation (3), it follows that the foam height needed for the total amount of liquid at time zero to be N times the final amount of liquid in the capillary profile is

$$H = 2\xi(N\varepsilon_C - \varepsilon_0)/\varepsilon_0 \quad (8)$$

where ε_0 is the initial liquid fraction and ε_C is the liquid fraction at the bottom of the foam. The heights for a factor of $N = 2$ are shown in Figure 2b, assuming $\varepsilon_C \approx 0.37$ as in the random close packing of spheres. The results

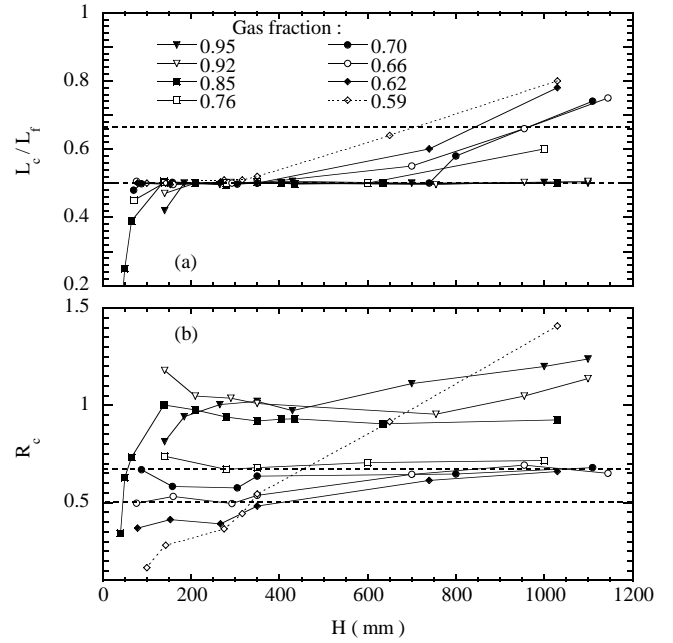


Fig. 5. (a) Dimensionless liquid height, $L_c/L_f = L(t_c)/L(\infty)$, and (b) dimensionless drainage rate, $R_c = d(L/L_f)/d(t/t_c)|_{t_c}$, at time the inflection time t_c vs. the height of the foam sample. In both plots, the dashed lines at $1/2$ and $2/3$ are, respectively, the predictions based on Plateau border-dominated and vertex-dominated dissipation, neglecting capillarity. As an aside, foams wetter than about 63% gas show qualitatively different trends in behavior since the bubbles are free to convect and rearrange.

correspond well to the point beyond which t_c/H becomes constant.

To complete the characterization of drainage vs. height and liquid content, we display in Figure 5a the dimensionless liquid height and drainage rate at the inflection time t_c . The former, L_c/L_f , behaves most simply for dry foams, equaling $1/2$ as long as the sample height is not too small. This agrees with the prediction of equation (6) for Plateau-border dominated dissipation. For wetter foams, $L_c/L_f = 1/2$ is found also; however, if the sample height is too large then the value increases. Rather than increase without bound for large H , the drainage rate approaches a maximum value and simply persists for longer as H is further increased. While the L_c/L_f data generally seem to indicate Plateau border-dominated dissipation, the corresponding dimensionless drainage rate $R_c = 1/2$ is not observed. Instead, the rate data plotted in Figure 5b are close to 1 for the same dry foams exhibiting $L_c/L_f = 1/2$. Furthermore, for the wetter foams, the dimensionless drainage rate is very close to the prediction $R_c = 2/3$ of equation (7) for vertex-dominated dissipation.

Conclusions

Using a new device to rapidly produce uniform foams, we obtained a comprehensive set of data on foam drainage

as a systematic function of both liquid content and sample height. Results were presented for the time dependence of the amount of drained liquid, $L(t)$; these were analyzed in terms of the characteristic time t_c at which the drainage rate becomes maximum, plus the concurrent dimensionless liquid height $L_c/L_f = L(t_c)/L(\infty)$, and the dimensionless drainage rate $R_c = d(L/L_f)/d(t/t_c)|_{t_c}$. Such data were compared with analytic predictions based on two versions of the drainage equation, assuming either Plateau border-dominated or vertex-dominated dissipation, and neglecting capillarity. Unfortunately, no simple story emerged. Significant aspects of all four quantities behaved differently from both predictions. For dry foams, the behavior of $L(t)$ at intermediate times and the value of L_c/L_f are both consistent with border-dominated dissipation, but the behavior of $L(t)$ at other times as well as the values of t_c and R_c are not. For wet foams, the behavior of $L(t)$ at intermediate times and the value of R_c are both consistent with vertex-dominated dissipation, but the behavior of $L(t)$ at other times as well as the values of t_c and L_c/L_f are not. For all foams, the level of agreement depends on the sample height. What can explain such behavior? While it is possible that neither dissipation mechanism, nor our specific assumptions about the film/border/vertex geometry, are valid over the full range of liquid content, a large source of the discrepancy must be the neglect of capillarity. Based on our experiments, we speculate that capillarity will influence free drainage under the following conditions. If the foam height is small enough that the total amount of liquid in the sample is not much greater than the amount of liquid remaining in the final equilibrium capillary profile, then it will be important at all times. Otherwise, capillarity will still be important at short times for dry samples, with liquid remaining entirely inside the foam for a finite period rather than draining out at constant rate immediately after production. And capillarity will still be important at late times for all samples, with liquid adjusting into the equilibrium capillary profile rather than emptying out altogether. Unfortunately, the inclusion of capillarity renders the drainage equations too nonlinear for analytic solution, requiring instead difficult numerical work. This appears necessary to further elucidate the nature of free drainage in foams. Hopefully, the comprehensive nature of our data, and our identification of key dimensionless quantities, will help to inspire and guide such a project.

We thank A.M Kraynik for helpful conversations; P.A. Kittle for design advice on the foam machine; S.A. Koehler and S. Hilgenfeldt, plus R.S. Ghaskadvi and M. Dennin, for sharing unpublished results; and NASA for support through grant NAG3-1419.

References

1. J.J. Bikerman, *Foams* (Springer-Verlag, New York, 1973).
2. D. Weaire, N. Rivier, *Contemp. Phys.* **25**, 55 (1984).
3. J.H. Aubert, A.M. Kraynik, P.B. Rand, *Sci. Am.* **254**, 74-82 (1989).
4. D.J. Durian, D.A. Weitz, *Foams*, in Kirk-Othmer *Encyclopedia of Chemical Technology*, 4th edn., edited by J.I. Kroschwitz (Wiley, New York, 1994), Vol. 11, pp. 783-805.
5. *Foams: Theory, Measurement, and Application*, edited by R.K. Prud'homme, S.A. Khan, Surfactant Sci. Ser. **57** (Marcel Dekker, NY, 1996).
6. A.M. Kraynik, *Ann. Rev. Fluid Mech.* **20**, 325-357 (1988).
7. A.D. Gopal, D.J. Durian, *Phys. Rev. Lett.* **75**, 2610-2613 (1995).
8. A.D. Gopal, D.J. Durian, *Shear-induced "melting" of an aqueous foam* (preprint submitted to *J. Coll. I. Sci.* 1998).
9. J.A. Glazier, S.P. Gross, J. Stavans, *Phys. Rev. A* **36**, 306-316 (1987).
10. D.J. Durian, D.A. Weitz, D.J. Pine, *Phys. Rev. A* **44**, R7902-R7905 (1991).
11. J.A. Glazier, D. Weaire, *J. Phys. Cond. Matter* **4**, 1867-1894 (1992).
12. J. Stavans, *Rep. Prog. Phys.* **56**, 733-789 (1993).
13. A. Bhakta, E. Ruckenstein, *Adv. Colloid Interface Sci.* **70**, 1-124 (1997).
14. D. Weaire, S. Hutzler, G. Verbist, E. Peters, *Adv. Chem. Phys.* **102**, 315-374 (1997).
15. D. Weaire, N. Pittet, S. Hutzler, D. Pardal, *Phys. Rev. Lett.* **71**, 2670-2673 (1993).
16. N. Pittet, P. Boltzenhagen, N. Rivier, D. Weaire, *Europhys. Lett.* **35**, 547-552 (1996).
17. S. Hutzler, D. Weaire, R. Crawford, *Europhys. Lett.* **41**, 461-465 (1998).
18. P.A. Sanders, *Handbook of Aerosol Technology*, 2nd edn (Van Nostrand Reinhold Company, New York, 1979).
19. J.F. Fry, R.J. French, *J. Appl. Chem.* **1**, 425-429 (1951).
20. J.J. Kroll, *Foam generating apparatus and method*, USA Patent No. 4,474,680 (1984).
21. P.A. Kittle, personal communication, Aquafoam Inc., <http://www.aquafoam.com/> (1997).
22. D.S.H. Sit Ram Sarma, J. Pandit, K.C. Khilar, *J. Coll. I. Sci.* **124**, 339-348 (1988).
23. M.V. Ramani, R. Kumar, K.S. Gandhi, *Chem. Eng. Sci.* **48**, 455-465 (1993).
24. R.J. Germick, A.S. Rehill, G. Narsimhan, *J. Food Eng.* **23**, 555-578 (1994).
25. A.R. Bhakta, K.C. Khilar, *Langmuir* **7**, 1827-1832 (1991).
26. A. Bhakta, E. Ruckenstein, *Langmuir* **11**, 1486-1492 (1995).
27. G. Verbist, D. Weaire, A.M. Kraynik, *J. Phys. Cond. Matter* **8**, 3715-3731 (1996).
28. I.I. Gol'dfarb, K.B. Kann, I.R. Shreiber, *Liquid flow in foams*, Fluid Dynamics (English translation of *Izv. Akad. Nauk SSSR*) **23**, 244-249 (1988).
29. G. Verbist, D. Weaire, *Europhys. Lett.* **26**, 631-634 (1994).
30. V. Goldshtein, I. Goldfarb, I. Shreiber, *Int. J. Multiphase Flow* **22**, 991-1003 (1996).
31. S.A. Koehler, H.A. Stone, M.P. Brenner, J. Eggers, *Phys. Rev. E* **58**, 2097-2106 (1998).
32. M. Gururaj, R. Kumar, K.S. Gandhi, *Langmuir* **11**, 1381-1391 (1995).
33. S.A. Koehler, S. Hilgenfeldt, H.A. Stone, *Experimental and theoretical investigations of fluid drainage in foams*, DFD abstract (1998, preprint should soon be available).
34. H.M. Princen, A.D. Kiss, *Langmuir* **3**, 36-41 (1987).
35. A.M. Kraynik, *Foam drainage report*, Sandia Report, SAND83-0844 (1983).
36. R.S. Ghaskadvi, M. Dennin, *Rev. Sci. Inst.* **69**, 3568-3572 (1998).
37. R.S. Ghaskadvi, M. Dennin (unpublished results, 1999).